AIChE WILEY InterScience DISCOVER SOMETHING GREAT

REACTORS, KINETICS, AND CATALYSIS

Optical and Infrared Study of Individual Reacting Metallocene Catalyst Particles

Phillip Hamilton, David R. Hill, and Dan Luss
Dept. of Chemical and Bimolecular Engineering, University of Houston, Houston, TX 77204

DOI 10.1002/aic.11415
Published online February 19, 2008 in Wiley InterScience (www.interscience.wiley.com).

Polymer particle agglomeration and melting causing sheet formation in fluidized bed reactors have been reported to occur during olefin polymerization. The cause of this deleterious sheet formation has not yet been established. Infrared and optical imaging were used to study the temporal temperature and size during polymerization of individual commercially active catalyst particles supported on a nylon mesh. Experiments conducted at 2100 kPa confirmed theoretical predictions that the temporal temperature rapidly attains a maximum after the start of the reaction. The magnitude of the temperature rise increases upon an increase of either reactor temperature, initial catalyst particle diameter, catalyst loading, or addition of hydrogen to the feed. The maximum transient temperature rise of single commercial catalyst particle during ethylene polymerization (7.5°C) is lower than that which can lead to local melting and polymer sheet formation. The temperature rise of particle clusters is much higher than that of individual particles, as the cluster acts as a particle with an effective diameter much larger than that of an individual particle. Thus, to circumvent polymer melting it is essential to avoid catalyst particles clustering, which may be caused by electrostatic attraction. The addition of hydrogen to the feed, often used to control polymer properties, significantly increased the initial particle temperature rise (almost double in some cases). © 2008 American Institute of Chemical Engineers *AIChE J,* 54: 1054–1063, 2008
Keywords: metallocene, catalysis, reaction kinetics, infrared imaging, polyolefin

Introduction

Many polyolefins are produced commercially by gas-phase polymerization in fluidized bed reactors using either metallocene, chromium oxide, or Ziegler–Natta catalysts. Metallocene catalysts provide control of the polymer structure and molecular weight, allowing tailoring of the polymers' physical properties.[1] Polymers produced by metallocene catalysts have a narrower molecular weight distribution than those produced using Ziegler–Natta catalysts.[2,3] Local overheating of the growing polymer particles can cause their softening or melting leading to particle agglomeration, which may require reactor shutdown.[4] Though highly exothermic polymerization reactions are well handled in gas phase fluid bed reactors, polymer particle melting and agglomeration has caused major operational problems (formation of polymer sheets) during gas-phase olefin polymerization.[5] The overall temperature rise in commercial reactors is controlled by operating at low per pass olefin conversion (order of 2%) and cooling of the recycled effluents. However, polymer sheet formation and the lack of advanced warning of such events remains a serious operational problem.[6] To circumvent polymer sheet formation, it is essential to gain an understanding of what can cause local temperature rise, and the dependence of its magnitude on the catalyst properties and the operating conditions. This information will enable a more rational design of new catalysts and of the operation procedure.

Simulations of a growing polymer particle indicate that a very rapid temperature rise occurs in the initial stages of

Correspondence concerning this article should be addressed to D. Luss at dluss@uh.edu.
Current address of Phillip Hamilton: Shell Global Solutions, Houston, TX 77007.
Current address of David R. Gill: The Dow Chemical Company, Freeport, TX 77541.

polymerization, which then decays.[7–10] Measurements of the temperature in a reactor containing many particles cannot determine the temperature rise on a single particle. This data can only be obtained by experiments in which the temporal temperature and size of a single particle are measured. The small size of the supported catalyst (order of 10–100 μm) requires use of a microscope to follow the temporal single particle size and an infrared camera to measure its temporal surface temperature. These measurements avoid physical contact with the particle and interaction with the reaction. Schmitz's group was the first to use infrared imaging to follow catalyst particle temperature.[11] It has since been used extensively to determine the temporal temperature on various catalysts[12,13] and in high throughput screening.[14] Weickert's group used infrared imaging to determine the temperature on growing polymer particles during propylene polymerization.[15–20]

We report here experiments we conducted to determine the magnitude of the temperature rise of individual supported metallocene catalyst particles and its dependence on the reactor temperature, initial catalyst particle size, and the addition of hydrogen to the feed. The experiments were conducted using commercial metallocene catalysts with activity in excess of 5000 g polymer/(g cat h).

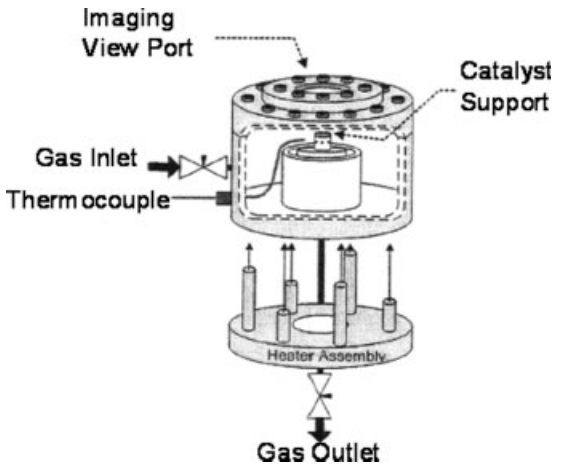

Figure 1. Schematic of the reactor used to image the growing polymer particles.

Experimental System

The experimental system used to measure the temporal temperature and size of individual metallocene catalyst particles during polymerization consisted of a reactor, gas delivery and purification system, and cameras. The reactor, shown schematically in Figure 1, is a cylindrical vessel with an ID of 5 cm and an inside height of 3.75 cm. An Omega CN9000 temperature controller keeps the bulk reactor temperature at the set point $\pm 0.5^{\circ}$C using six body mounted cartridge heaters. A fan cools the outside of the reactor and prevents heating of the infrared lens. A few separated catalyst pellets were placed on a 25-μm mesh nylon grid stretched across an open cylindrical pedestal in the center of the reactor. The low thermal conductivity and heat capacity of the nylon support minimizes the attenuation of the particle temperature due to heat transfer to the support.

A thin (1/8 in.) optical grade sapphire window, which has a high transmittance for infrared radiation in the 3- to 5-μm wavelength range, is installed in the lid of the reactor. It can withstand 3100 kPa pressure at 120°C and is positioned directly above the catalyst support. The reactor body houses a pedestal on which the catalyst is placed and a thermocouple that measures the reactor temperature. The hollow pedestal serves as the exit port for the reactant gases and is surrounded by a trough filled with silica-supported methyl aluminoxane and a small amount of excess catalyst as a guard bed to adsorb poisons before they reach the target catalyst particles.

The reactor is fed with highly purified ethylene, propylene, butene, and/or hydrogen. As the experiments utilize just a few particles, even trace amounts of contaminants can deactivate them. The metallocene catalysts used in the experiments are very susceptible to poisoning from oxygen, water, or CO. The feed gases contain less than 1 ppm of these poisons.

The catalyst particle growth rate is measured by an optical microscope objective attached to a Sony DSP 3CCD (Model number DXC-390) color video camera, using a computer to record an image every second. In each visual image, the particle size is determined using customized software, which uses edge detection principles to determine the size of the catalyst in each frame. The optical microscope is focusable from infinity to a 9-mm front working distance and has a resolution of 1.3 μm per pixel, which is $\sim$2.5% of the catalyst average initial size.

The surface temperature of the growing particle is measured by an Indigo Systems Merlin Mid infrared camera (Model number 414-0001-90), which measures infrared radiation in a wave length range of 3–5 μm. It can accurately measure temperature variations within 0.1°C. The transmission of the sapphire window in this range is 80–85%, so that the radiation flux reaching the camera is attenuated by 15–20%. The curvature of the particle causes the luminance over the particle surface to be nonuniform, even when the particle temperature is uniform. To circumvent this problem, the particle temperature is measured by averaging the reading from at least 5–10 pixels from the center of the particle, from which the emissivity is rather insensitive to curvature effects. An external emissivity correction is applied to distinguish between the radiation of the background and the polymer particle.

Before conducting any polymerization run, a calibration curve of the radiation dependence on the surface temperature was determined by 14 experiments. The particle surface temperature data were obtained from several runs, with multiple single particles followed, when possible, in each successful experiment. The visual and infrared thermographic images of the growing metallocene catalyst particles were acquired in 1 s intervals for a period between 5 and 10 min, as the particle temperature rise is most significant in the first few minutes after starting the reaction.

The experiments were conducted using three commercial high activity catalysts. TT-1 and TT-2 are ethylene polymerization catalysts and D-1 is a propylene polymerization catalyst. Propriety restrictions prevent us from providing information on the catalyst structure, properties, or composition. The experiments were carried out to determine the depend-

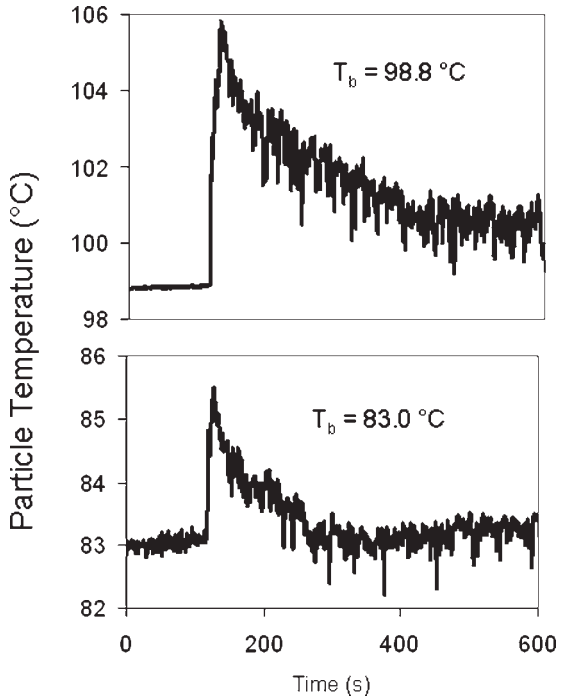

Figure 2. The temporal temperature of two catalyst particles TT-1 at two different reactor temperatures (a) 83.0°C (b) 98.8°C.

ence of the particle temperature and size on the reactor temperature, addition of hydrogen to the feed, initial catalyst particle size, and clustering of particles.

Impact of Reactor Temperature

Experiments using catalyst TT-1 were conducted to determine the impact of the reactor temperature on the particle temperature profile. The reactant gas mixture of 93.00% ethylene, 6.96% butene, and 0.04% hydrogen is similar to that used industrially with this catalyst. The initial diameter of each particle in these experiments was ~50 μm. The reactor pressure was 2100 kPa.

The experiments showed that the reactor temperature had a strong impact on the magnitude of the particle temperature rise. Figure 2 shows the temperature of a catalyst particle for two cases. In one, the reactor temperature was 83.0°C, in the second it was 98.8°C. The maximum temperature rise on the particle at a reactor temperature of 98.8°C (7.2°C) is considerably higher than that at 83.0°C (2.5°C). The time required to reach the maximum temperature rise was rather similar for both cases (within 2 s of each other).

Experiments conducted at different reactor temperatures (Figure 3) show that the peak temperature was a monotonically increasing function of the reactor temperature, as predicted by mathematical models.[7–10] Numerical simulations suggest that the activation energy of the propagation reaction is the main factor affecting the dependence of the peak temperature rise on the reactor temperature. The peak temperature rise for catalyst TT-1 increased by 1°C as the reactor temperature increased by 4°C over the range of 80–100°C.

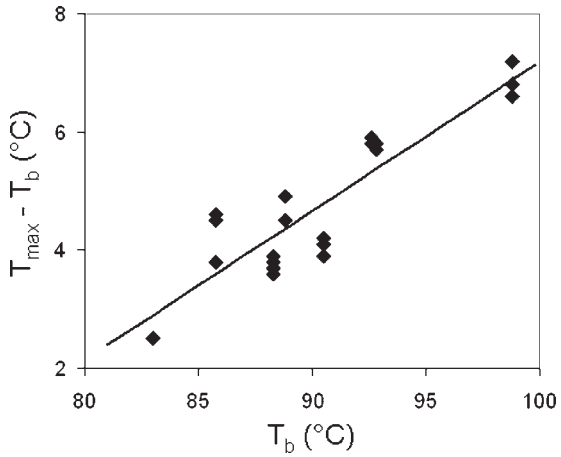

Figure 3. Dependence of maximum temporal temperature rise on reactor temperature for catalyst TT-1.

The visual camera was used to determine the effect of reactor temperature on the temporal particle diameter. Typical dimensionless temporal growing particle volumes (ratio between temporal volume and initial volume) are shown in Figure 4 at three different reactor temperatures (80, 85, and 88°C). The initial diameter of each particle in these experiments was ~50 μm, and the feed was pure ethylene. The reactor pressure was 2100 kPa. The figure shows that the dimensionless volume at any time was larger at the higher reactor temperatures. To determine the rate of volume growth, a fourth order polynomial was fit to the data in Figure 4 and the derivatives were taken as the dimensionless growth rate for the particles. Figure 5 shows that the higher the reactor temperature, the larger is the maximum particle growth rate. For TT-1, increasing the bulk temperature from 80 to 88°C increased the maximum growth rate by 58%. The maximum growth rate for each of the three reactor temperatures was attained at about 47 s after the start of the reaction. In all the three cases, the growth rate decreased from its maximum to a local minimum and then increased to a

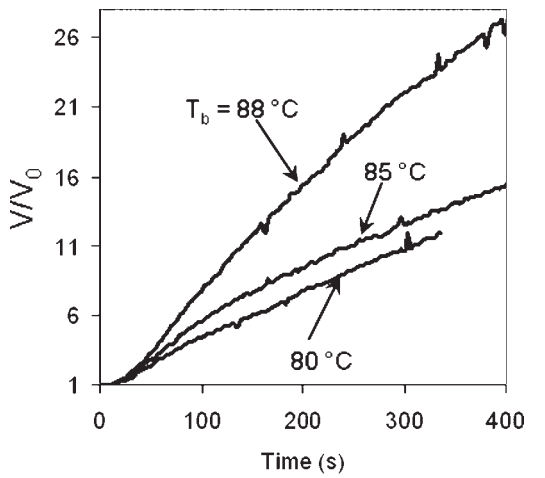

Figure 4. Temporal dimensionless growing particle volume using catalyst TT-1 at reactor temperatures of 80, 85, and 88°C.

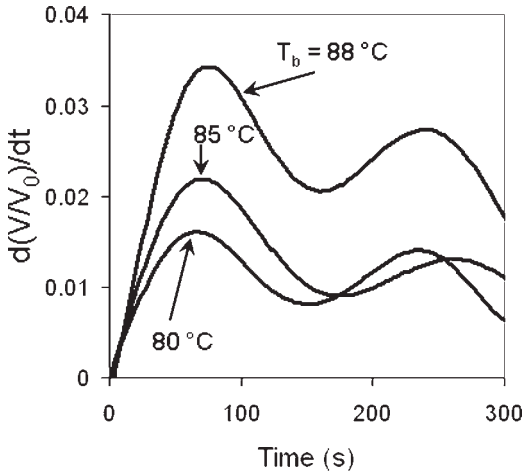

Figure 5. Dependence of temporal polymer particle growth rate on the reactor temperature using catalyst TT-1 at reactor temperatures of 80, 85, and 88°C.

shallow maximum. The existence of a local minimum in the volumetric growth rate is not predicted by existing mathematical models.[7–10]

Effect of Hydrogen Addition

Hydrogen is a chain transfer agent used to control the polymer molecular weight. With Ziegler–Natta catalysts, this usually decreases the catalyst activity.[21,22] However, for metallocene catalysts addition of hydrogen increases the catalyst activity, and hence the reactor production rate for a given catalyst feed rate. The hydrogen forms a hydride with the catalyst metal center that rapidly reacts with olefins, forming a growing polymer chain.[23] The hydrogen increases the rate constant of the chain initiation reaction in a way similar to that of a cocatalyst. This, in turn, increases the initial particle temperature rise. Hydrogen addition is used to control the polymer molecular weight, because of its interaction with the active metal center. Although the addition of one hydrogen atom to the end of a growing polymer chain terminates its growth, the second hydrogen atom bonds to the metal center forming a hydride that rapidly initiates a new polymer chain.[24]

The addition of hydrogen to the feed in experiments conducted with catalyst from batch TT-2 increased the maximum particle temperature rise over that obtained using a pure ethylene feed. Figure 6 describes the temperature profile for two cases (reactor temperatures of 82 and 85°C) using a feed of 100% ethylene and a pressure of 2100 kPa. The initial particle diameter in both cases was essentially the same. As in the case shown in Figure 2, the maximum temperature rise was obtained shortly after the start of the reaction, and a higher temperature rise occurred as the reactor temperature was raised.

The transient temperature profiles for the same two reactor temperatures but for a feed containing 99.96% ethylene and 0.04% hydrogen is shown in Figure 7. A comparison of Figures 6 and 7 shows that at a reactor temperature of 82°C the temperature rise for the pure ethylene case was 3.7°C, while

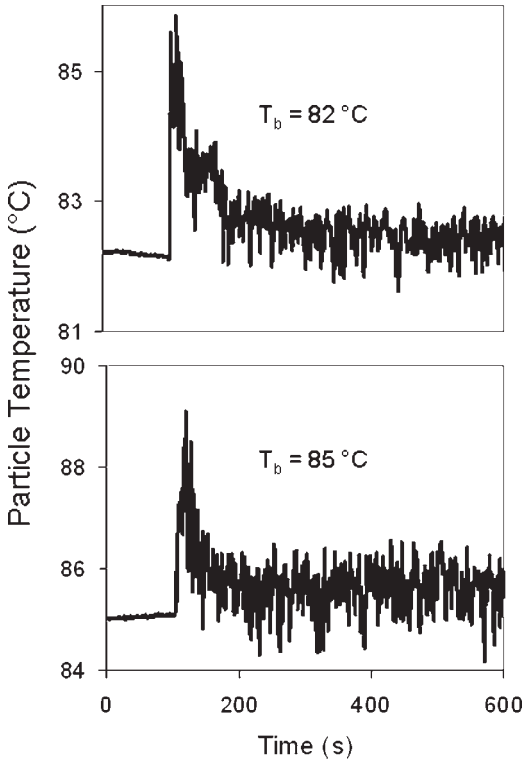

Figure 6. Temporal temperature for two TT-2 catalyst particles with pure ethylene as the feed gas.

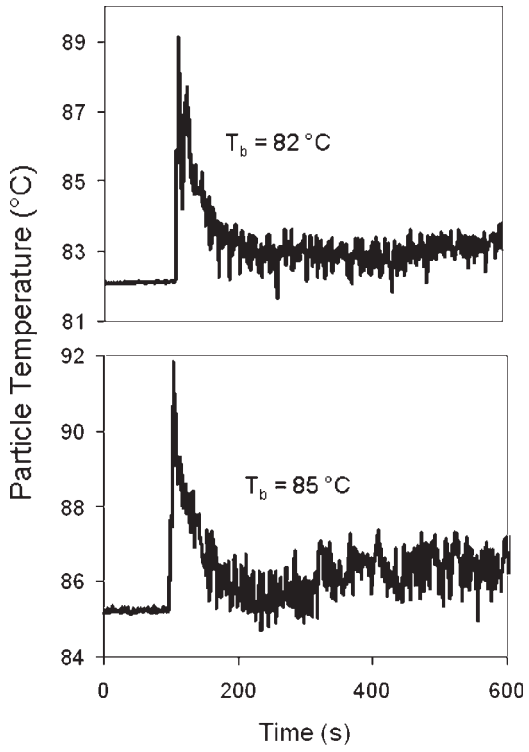

Figure 7. Temporal temperature for two TT-2 catalyst particles with 99.96% ethylene and 0.04% hydrogen as the feed gas.

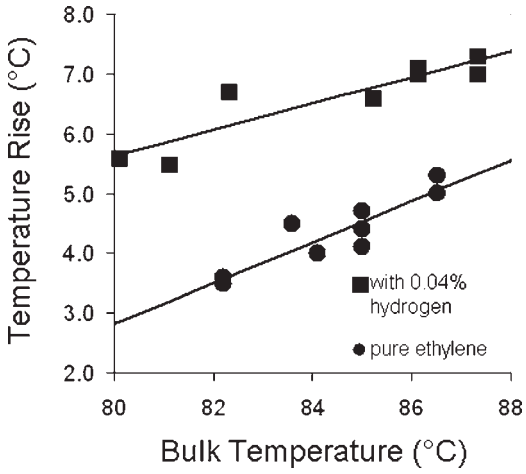

Figure 8. Comparison of the maximum temporal temperature rise as function of the reactor temperature for TT-2 catalyst particles with a feed of (a) pure ethylene and (b) ethylene containing 0.04 vol % hydrogen.

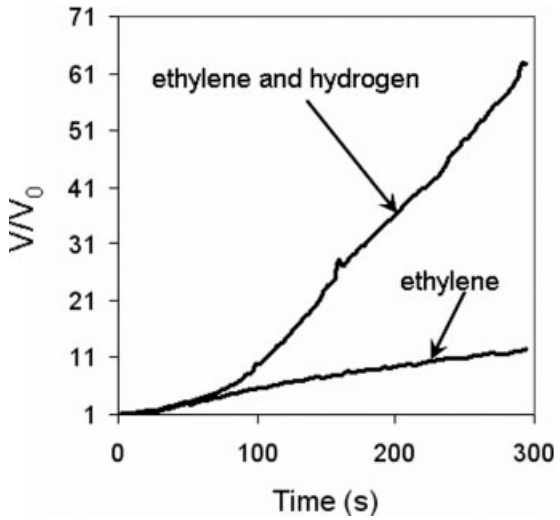

Figure 9. Comparison of the temporal dimensionless volume of TT-2 catalyst particles for a feed of pure ethylene and of ethylene containing 0.04 vol % hydrogen, reactor temperature of 85°C.

the addition of a small amount of hydrogen (0.04 vol %) to the feed led to a temperature rise of 7.0°C. In the experiments conducted at 85°C, the temperature rise for the feed with hydrogen was 6.8°C, while for the pure ethylene feed it was only 4.1°C. Additional experiments (Figure 8) show that the addition of a small amount of hydrogen to the ethylene feed increased the temperature rise for all reactor temperatures between 80 and 88°C.

The addition of hydrogen accelerated the rate at which the peak temperature was reached. On the average, the addition of hydrogen to the reactant gas reduced the time required for the particle to reach its maximum temperature to one-third that for a feed of pure ethylene. For example, the peak temperature was reached within 3.8 s on average using a feed of ethylene and hydrogen compared to 11.9 s on the average using pure ethylene feed. Previous academic experimental studies on the impact of hydrogen in large batch experiments revealed similar behavior.[25] For the feed containing hydrogen, the particle transient temperature formed a local minimum and then increased slightly forming a small local maximum at about 300 s after the start of the reaction.

The visual camera was used to determine the effect of the addition of hydrogen to the reactant gas on the particle growth. Figure 9 shows the temporal dimensionless volume (V/V_0) for two TT-2 particles each at a reactor temperature of 85°C and a total pressure of 2100 kPa. The initial diameter of these particles was ~50 μm. Because of agglomeration among different growing particles, we show only data for the first 300 s. The difference in these two experiments is that one was conducted with a feed of pure ethylene and the second for a feed with 0.04% hydrogen. The hydrogen addition led to a faster initiation of the polymerization and faster rate of particle growth. The volume of the particle exposed at 85°C to ethylene containing hydrogen was more than eight times larger than that of the particle exposed to pure ethylene within 5 min after initiation of the reaction.

Figure 10 shows the temporal dimensionless particle growth rate for the two experiments described in Figure 9. A fourth order polynomial was fit to the data, and its derivatives were taken as the dimensionless growth rate for the particles. When hydrogen was added to the reactant gas, the growth rate of the particle initially increased and attained a local maximum. It then decreased and reached a local minimum at about 250 s after the start of the reaction. It then increased for a while reaching a shallow maximum. The growth rate for the particle with pure ethylene as the feed gas exhibited the same qualitative features. However, except for the initial period, its growth rate was much smaller than that of the feed containing hydrogen. Comparison of Figure 10 with Figure 7 indicates that the maximum in the temperature rise occurs ahead of the maximum in the particle growth rate.

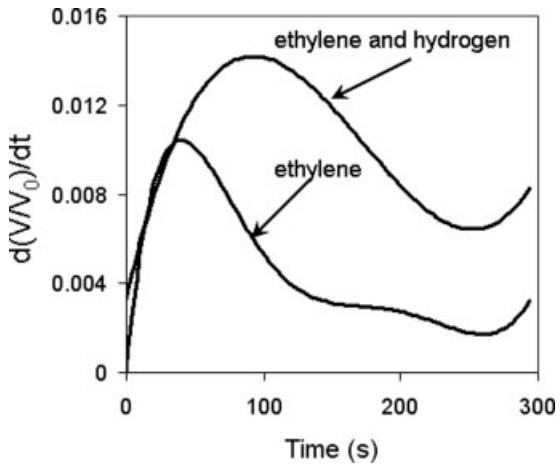

Figure 10. Temporal dimensionless volume growth rate of TT-2 catalyst particle for a feed of pure ethylene and of ethylene containing 0.04 vol % hydrogen, reactor temperature of 85°C.

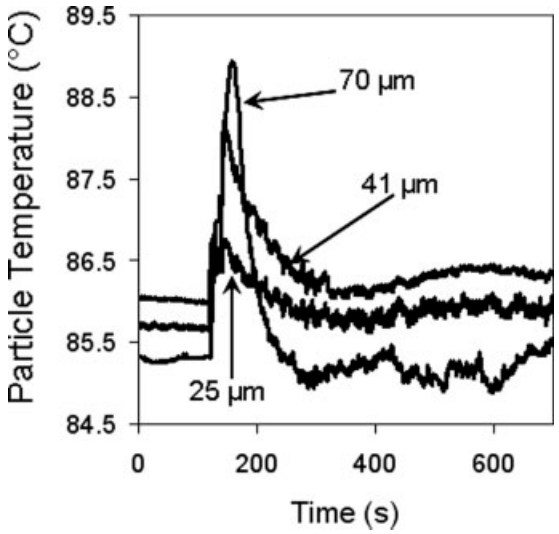

Figure 11. Dependence of the temporal temperature on the initial size of a single D-1 catalyst particle.

Feed containing 93 vol % propylene and 7 vol % hydrogen, reactor pressure 700 kPa.

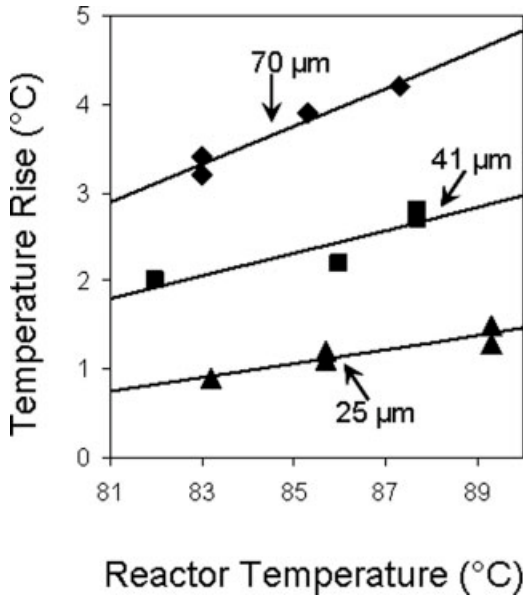

Figure 12. Dependence of the maximum temporal temperature on the reactor temperature for D-1 catalyst particles of three different sizes.

Feed containing 93 vol % propylene and 7 vol % hydrogen, reactor pressure 700 kPa.

Effect of Initial Particle Size

Model simulations predict that the initial particle size strongly affects the magnitude of the initial temperature rise as it affects the initial ratio of surface area to volume.[7–10] To test these predictions, we conducted the polymerization of propylene using catalyst D-1 with initial support diameters of 25, 41, and 70 μm. The feed to the reactor was 93 vol % propylene and 7 vol % hydrogen, and the pressure was 700 kPa.

The transient temperature for three different initial particle sizes are shown in Figure 11 for experiments conducted at about 85.5°C. As in ethylene polymerization, a temperature peak was obtained shortly after the start of the reaction. The maximum transient temperature rise at a reactor temperature of 85.5°C was 1.1, 2.2, and 3.9°C for particles with an initial diameter of 25, 41, and 70 μm, respectively. This trend is in agreement with model predictions of the increase in the peak temperature rise with particle size.[7–10] Additional experiments with reactor temperatures over the range of 80–90°C, shown in Figure 12, verify this trend. Over this range (80–90°C), the average particle peak temperature rise was 1.2, 2.3, and 3.7°C for particles with an initial diameter of 25, 41, and 70 μm, respectively.

The metallocene loading of the three commercial polypropylene catalysts were slightly different (~15%). However, for proprietary reasons we cannot disclose these values. The initial catalyst support diameters were 25, 41, and 70 μm, respectively. Modeling suggests that the dominant factor determining the dependence of the peak temperature rise on the particle diameter is, ϕ_p, the Thiele modulus of the propagation reaction,[7–10] defined as:

$$\phi_p = R(0)\sqrt{\frac{k_p(T_b)C^0(0)}{D_e}}, \qquad (1)$$

where $R(0)$ is the initial particle diameter. Figure 13 describes the dependence of the average temperature rise on the relative Thiele modulus, defined as

$$r(\phi_{p_i}) = \frac{\phi_{p_i}}{\phi_{p_1}} = \frac{R(0)_i\sqrt{\text{Loading}_i}}{R(0)_1\sqrt{\text{Loading}_1}} \qquad i = 1, 2, 3, \qquad (2)$$

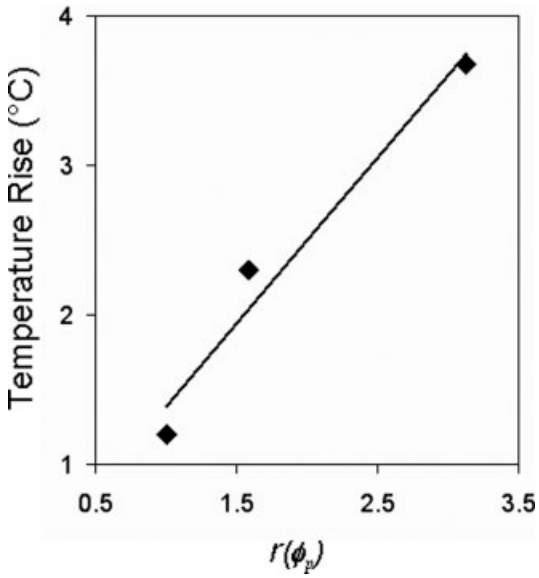

Figure 13. Dependence of the maximum temperature rise of D-1 catalyst particle on ϕ_p.

Feed containing 93 vol % propylene and 7 vol % hydrogen, reactor pressure 700 kPa.

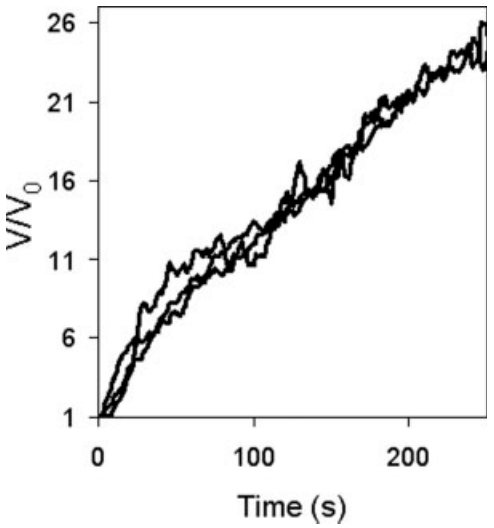

Figure 14. Temporal dimensionless volume of three D-1 catalyst particles ranging in diameter from 25 to 70 μm.

Feed containing 93 vol % propylene and 7 vol % hydrogen, reactor temperature of 85.5°C and 700 kPa pressure.

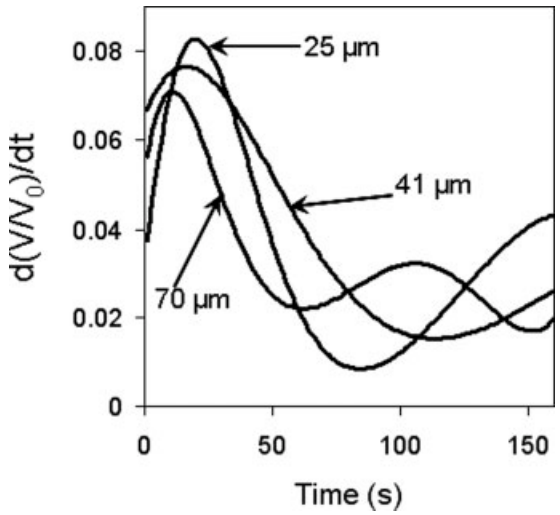

Figure 15. Temporal dimensionless particle growth rate of three D-1 catalyst particles of different sizes.

Feed containing 93 vol % propylene and 7 vol % hydrogen, reactor temperature of 85.5°C and 700 kPa pressure.

where the subscripts 1, 2, and 3 refer to particles with an initial diameter of 25, 41, and 70 μm, respectively. The relative moduli for these three particles are 1, 1.6, and 3.1, respectively. Figure 13 shows that the average temperature rise is a linear function of the relative Thiele modulus of the propagation reaction, which is in agreement with model predictions by Hamilton et al.[9,10] for low to moderate values of ϕ_p (0.5–3). The model predicts that for large ϕ_p values, the maximum temperature rise is larger than a linear function of ϕ_p.

The visual camera was used to determine the transient particles size using the same catalysts and operating conditions as those shown in Figure 11. Figure 14 shows, within experimental errors, the temporal dimensionless volume (V/V_0) at a reactor temperature of 85°C was independent of the initial particle size. This result is in agreement with previous experiments by Pater et al.[20]

The rate of the particle volume growth was computed by fitting a fourth order polynomial to the data in Figure 14. The derivatives of these polynomials were taken as the dimensionless growth rate for the particles. The relative small differences in the rate of volume growth for the three particles (Figure 15) may be due to experimental errors and slight differences in the reactor temperature. The initial maximum in the rate was obtained after the temperature peak formed. In all the experiments, a shallow local minimum in the growth rate was obtained after the initial maximum.

Effect of Particle Clusters

A potentially significant operation problem in fluidized bed polymerization reactors, is the clustering of catalyst particles either as they are injected into the bed or due to the build up of electrostatic charges. To study the impact of catalyst clustering, experiments were carried out in which clusters of catalyst particles were placed on the screen in our microreactor. Figure 16 shows the results of experiments, conducted at reactor temperature of 93°C and total pressure of 2100 kPa, using catalyst from batch TT-2. The reactant feed composition was 93.00 vol % ethylene, 6.96 vol % butene, and 0.04 vol % hydrogen. Under these conditions,

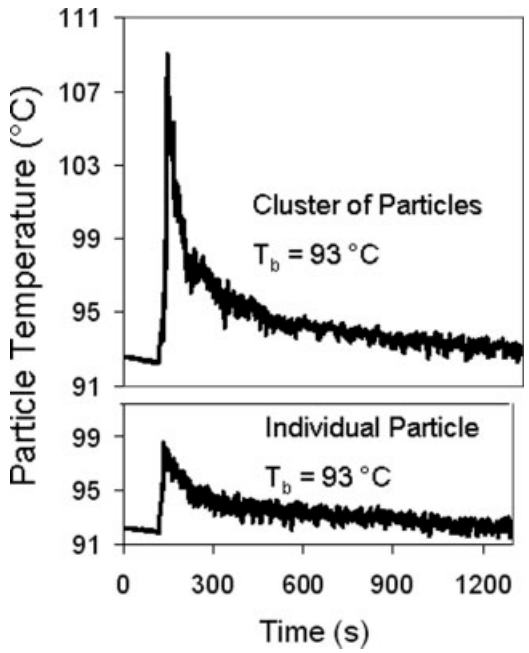

Figure 16. Comparison of the temporal temperature of a single TT-2 catalyst particle to that of a cluster of particles at a reactor temperature of 93°C.

Feed of 93.0 vol % ethylene, 6.96 vol % butene, and 0.04 vol % hydrogen, pressure of 2100 kPa.

the peak temperature rise for a single particle was 6.3°C, while that of particle cluster was 16.4°C. This is an increase of 10.1°C or 161% of the maximum transient temperature rise. These experiments show that when particles stick together the maximum temperature rise is much higher than that on single particles.

Discussion of Results

The experiments showed that the particle temperature reached a peak shortly after the start of the reaction then decays. This behavior agrees with model predictions[7–10] as well as with previous measurements reported by Weickert's group.[19,20] The magnitude of this peak temperature increases as the ambient temperature (Figures 2 and 3) or the particle size increases (Figures 11 and 12). Pater et al.[20] also observed an increase in the peak temperature as the initial particle size was increased. Our experiments are the first to show a large increase of the peak temperature upon addition of hydrogen to the gaseous reactants mixture (Figure 8). Pater et al.[20] reported a similar increase in the peak temperature upon the addition of a comonomer to the reactant gas. Clearly, increasing the loading of the catalyst and cocatalyst, which increases the propagation rate constant and the productivity of the catalyst particle, will also increase the temperature peak. The magnitude of this peak temperature can be reduced by prepolymerization, as it decreases the initial polymerization rate.

The temperature peaks generated by the three commercial catalysts we used were too low to cause melting or softening during the polymerization of single particles. This may, however, occur using larger catalyst particles or more active ones. We observed melting of growing polymer particles in some experiments when excess catalyst was loaded on the screen, so that the particles were not separated from each other. The clustering of individual particles led to a temperature peak much higher than that of a single particle (Figure 16). The reason being that a cluster acts as a single particle having an effective size much larger than that of the individual particles. Particles clustering may occur in a fluidized bed reactor due to electrostatic attraction among particles. Fine particles may form in a fluidized bed reactor either due to fragmentation or formation of polymer "fingers" on the particle surface, which break off upon collision with other particles. Electrostatic charge is most likely to build up on these fine particles in the dry environment. Various additives may be used to minimize the formation of electrostatic charges that can create such clusters. Their addition may help circumvent the undesired sheet formation.[26]

In all experiments, the temporal growth rate reached a maximum value shortly after the start of the reaction. After that it decreased to a local minimum and then increased to a shallow maximum (Figures 5, 10, and 15). This formation of a local minimum is surprising and is not predicted by literature models of single particle polymerization.[7–10] Similar behavior has already been observed by Pater et al.[20] We conjecture that fragmentation of the growing particle caused this small increase in the particle dimensionless volume growth rate after the minimum was attained. This fragmentation led to a temporary increase in the exposed active sites which, in turn, increased the reaction rate.

The magnitude of the temperature peak for a given feed is affected most strongly by the propagation rate constant. Determination of the peak temperature under several reactor temperatures enables, after use of some simplifying assumptions, estimation of the activation energy of the propagation reaction. The energy balance of a growing particle is,

$$\frac{d(\rho_p c_p T_p V_p)}{dt} = h_f S_p (T_b - T_p) + (-\Delta H) V_p R, \tag{3}$$

where R_p denotes the rate of the polymer growth. When the temporal particle temperature reaches its maximum $dT/dt = 0$. Assuming that the term describing the particle volume growth rate is small relative to that of the other term in Eq. 3 we get

$$(-\Delta H) V_p R \sim h_f S_p (T_p - T_b). \tag{4}$$

Assuming that the temporal temperature maximum is attained when all the particles have a similar size, we get that the relative reaction rates are defined by

$$r_i(T) = \frac{R_{pi}}{R_{p1}} = \frac{(T_{max_i} - T_{b_i})}{(T_{max_1} - T_{b_1})}, \tag{5}$$

where $T_{max,i}$ refers to the temperature peak obtained when the reactor temperature is $T_{b,i}$. Thus, the slope of $\ln[r_i(T)]$ vs. $1/T_{max}$ yields an approximate value of the activation energy of the propagation reaction. The value is just an approximation due to the simplifying assumptions described above and the fact that the concentration of the active sites, $\overline{C^*}$, may differ among the various particles. Figure 17 shows the relative rate was essentially a linear function of $1000/T_{max}$. The corresponding activation energy is 49 kJ/mol.

A comparison of Figures 6 and 7 with Figures 5 and 10 indicates that the maximum growth rate occurs after the maximum temperature has been attained. This is caused by the fact that by the time the peak temperature is attained, the fraction of the initial sites that are active is smaller than those at the time the maximum rate is obtained. To demonstrate this point, we present in Figure 18, a simulation of a typical case using the model described by Hamilton and

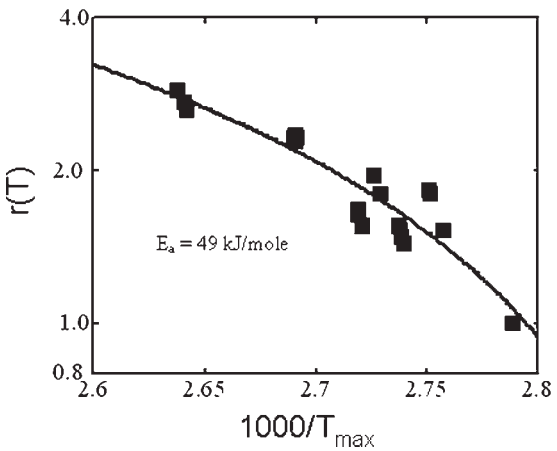

Figure 17. The dependence of *r(T)* on the inverse absolute temperature for TT-1 catalyst.

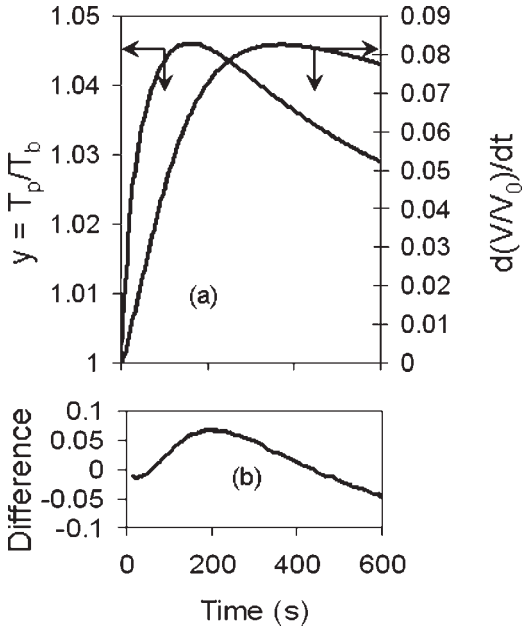

Figure 18. Simulation results demonstrating that (a) the peak in particle growth rate occurs after the peak in the particle temperature and (b) the close correlation between the growth rate and the number of active sites.

The parameter values used for the simulation are: ϕ_p = 3.4, ϕ_i= 0.02, ϕ_d = 0.005, γ_p = γ_i = 12, and γ_d = 10.

Luss.[10] Figure 18a demonstrates the model prediction that the temperature peak occurs prior to the peak in the particle growth rate. The simulations (Figure 18b) show that the dimensionless rate of particle growth is strongly connected to that of the fraction of the initial sites that are active. Figure 18b shows that a rather small difference exists between the normalized number of active sites (ratio of number of active sites to the maximum number of active sites) and the normalized particle growth rate (ratio of the particle growth rate to the maximum particle growth rate). When the peak transient temperature is obtained, the normalized number of active sites is 0.60 while it is 0.83 when the maximum growth rate is obtained. The particle temperature declines after the peak temperature is obtained, even though the overall reaction rate still increases. This occurs because the relative increase in the particle surface area and the corresponding heat loss exceeds the increased heat generation by the increasing reaction rate.

Conclusions

Increasing the reactor temperature increases the reaction rate and the peak temperature rise. Although the maximum temporal particle temperature rise (for catalyst D-1) increased linearly with the initial catalyst particle size, the corresponding dimensionless growth rate was, within experimental accuracy, independent of the initial particle size. The maximum observed temperature rise during polymerization on the three different commercially active single catalyst pellets (7.5°C) is too low to cause polymer melting. However, melting may occur on either larger or more active single catalytic pellets.

The largest initial temperature rise was observed on clusters of catalyst particles, which act as a particle with an effective diameter much larger than that of an individual particle. We conjecture that sheet formation due to local overheating in polymerization reactors may be caused by clustering of particles due to electrostatic attraction as frictional contact between particles can generate charges in a dry environment. Another possibility is that some particles have a very high activity as due to nonuniform loading they contain a higher concentration of metallocene than the bulk sample average. Elimination of these undesired effects should minimize the potential of sheet formation. Several patents claim that the frictional electrostatic charge build-up may be neutralized by various additives.[26] Prepolymerization of the catalyst particles will also decrease the magnitude of the initial temperature rise.

The addition of hydrogen, which is used as a chain transfer agent to control the molecular weight of the polymer, increases the productivity of the catalyst and the peak temperature rise. Thus, its addition increases the potential of local particle overheating. This may result in melting and particles sticking to the reactor wall or to each other. Hence, it is essential to check that the addition of the hydrogen will not lead to an excessive high temperature peak. The addition of hydrogen requires a trade-off between polymer property control and increased production rates to the need to avoid too high levels of overheating leading to sheet formation.

Acknowledgments

The authors are thankful to the ACS-PRF for financial support. Special thanks are due to Michael E. Muhle and Gaffar Vadgama of ExxonMobil, Tim Lynn and Jack Coalter of The Dow Chemical for helpful suggestions about the reactor design, and to Mike Townsley and Christian Uehara for developing the particle size tracking software.

Notation

C^0 = concentration of catalyst sites, mol/cm^3
C_p = heat capacity of polymer particle, J/(mol K)
C^* = active-sites concentration, mol-sites/cm^3
D_e = monomer effective diffusivity, cm^2/s
h_f = heat-transfer coefficient, J/(cm^2 s K)
$-\Delta H$ = heat of polymerization, J/mol
k_p = polymerization reaction rate, cm^3/(mol-sites s)
R = particle radius, μm
S_p = Surface area of particle, cm
t = time, s
T = temperature, K
T_p = temperature of particle, K
V_p = volume of particle, cm^3

Greek letters

ρ_p = particle density, g/cm^3
ϕ = nonisothermal Thiele modulus, defined by Ref. 10

Subscripts

b = ambient
f = final
i = initiation
max = maximum value

Literature Cited

1. Kaminsky W. New polymers by metallocene catalysis. *Macromol Chem Phys*. 1996;197:3907–3945.
2. Bubeck RA. Structure-property relationships in metallocene polyethylenes. *Mater Sci Eng R*. 2002;39:1–28.
3. Ray H. Polymerization Reaction Engineering V Conference, Quebec City, PQ, 2003.
4. Xie T, McAuley K, Hsu J, Bacon D. Gas phase ethylene polymerization: production processes, polymer properties, and reactor modeling. *Ind Eng Chem Res*. 1994;33:449–479.
5. Rotman D. Metallocene polyolefins: commodity capacity is a reality. *Chem Week*. 1997;159:20–23.
6. Hutchinson R, Ray WH. Polymerization of olefins through heterogeneous catalysis—the effect of condensation cooling on particle ignition. *J Appl Polym Sci*. 1991;43:1387–1390.
7. Song H, Luss D. Bounds on operating conditions leading to melting during olefin polymerization. *Ind Eng Chem Res*. 2004;43:270.
8. Song H, Luss D. Impact of initiation and deactivation on melting during gas-phase olefin polymerization. *Ind Eng Chem Res*. 2004;43:4789.
9. Hamilton P, Song H, Luss D. Dual-site supported metallocene catalyst design for bimodal polyolefin synthesis. *AIChE J*. 2007;53:687–694.
10. Hamilton P, Luss D. Metallocene catalyst design for optimum productivity. *Ind Eng Chem Res*. 2008.
11. Pawlicki PC, Schmitz RA. Spacial effects on supported catalysts. *Chem Eng Prog*. 1987;83:40–45.
12. Marwaha B, Luss D. Formation and dynamics of a hot zone in radial flow reactor. *AIChE J*. 2002;48:617–624.
13. Marwaha B, Luss D. Hot zones formation in packed bed reactors. *Chem Eng Sci*. 2003;58:733.
14. Moates FC, Somani M, Annamalai J, Richardson JT, Luss D, Willson RC. Infrared thermographic screening of combinatorial libraries of heterogeneous catalysts. *Ind Eng Chem Res*. 1996;35:4801–4803.
15. Weickert G, Meier GB, van Swaaij WPM. The particle as microreactor: catalytic propylene polymerizations with supported metallocenes and Ziegler-Natta catalysts. *Chem Eng Sci*. 1999;54:3291–3296.
16. Meier GB, Weickert G, van Swaaij WPM. FBR for catalytic propylene polymerization: controlled mixing and reactor modeling. *AIChE J*. 2002;48:1268–1283.
17. Samson J, Middelkoop B, Weickert G, Westerterp K. Gas-phase polymerization of propylene with a highly active Ziegler-Natta catalyst. *AIChE J*. 1999;45:1548–1558.
18. Roos P, Meier GB, Samson J, Weickert G, Westerterp K. Gas phase polymerization of ethylene with silica-supported metallocene catalyst: influence of temperature on deactivation. *Macromol Rapid Commun*. 1997;18:319–324.
19. Meier GB, Weikert G, Van Swaaij WPM. Gas-phase polymerization of propylene: reaction kinetics and molecular weight distribution. *J Polym Sci Part A: Polym Chem*. 2001;39:500.
20. Pater J, Weickert G, van Swaij, W. Optical and infrared imaging of growing polyolefin particles. *AIChE J*. 2003;49:450–464.
21. Kou Bo, McAuley K, Hsu C, Bacon D, Zhen Yao K. Gas-phase ethylene/hexene copolymerization with metallocene catalyst in a laboratory-scale reactor. *Ind Eng Chem Res*. 2005;44:2443–2450.
22. Blom R, Dahl I. Semi-batch polymerisation of ethylene with single-site catalysts in the presence of hydrogen. *Macromol Chem Phys*. 2001;202:719–725.
23. Casty G, Matturro M, Myers G, Reynolds R, Hall R. Hydrogen/deuterium exchange kinetics by a silica-supported zirconium hydride catalyst: evidence for a σ-bond metathesis mechanism. *Organometallics*. 2001;20:2246–2249.
24. Zdravkovski D, Miletti MC. Theoretical analysis of transition states in exchange reaction of hydrogen and methane involving σ-bond metathesis. *J Coord Chem*. 2006;59:777–782.
25. Soares JBP, Hamielic AE. Kinetics of propylene polymerization with a non-supported Ziegler-Natta catalyst—effect of hydrogen on rate of polymerization, stereo regularity, and molecular weight distribution. *Polymer*. 1996;37:4607–4614.
26. Good MG, Hasenberg DM, Spriggs TJ. Method for reducing sheeting during polymerization of α-olefins. US Pat 4,803,251, 1989.

Manuscript received Aug. 24, 2007, and revision received Nov. 20, 2007.